







# DFT/TD-DFT investigations on photovoltaic properties of *N*-Phenyl-*N*-(thiophen-2-yl)-1*H*-Pyrrol-2-amine and *N,N*-diphenylthiophen-2-amine based hexatriyne-thiophene dye-sensitizers for DSSCs

Kehinde Gabriel Obiyenwa<sup>1</sup> , Abimbola Modupe Olatunde<sup>2</sup> , Dayo Felix Latona<sup>3</sup> ,  
Willaim Ojoniko Anthony<sup>1</sup> , Pelumi Gabriel Adebayo<sup>4</sup>  and Banjo Semire<sup>1,4</sup>  

<sup>1</sup>Department of Chemistry, Federal University, Lokoja, Kogi State, Nigeria

<sup>2</sup>Department of Chemistry, University of Ibadan, Ibadan, Oyo state, Nigeria

<sup>3</sup>Department of Pure and Applied Chemistry, Osun State University, Osogbo, Nigeria

<sup>4</sup>Department of Pure and Applied Chemistry, Ladoke Akintola University of Technology, Ogbosomo, Nigeria

 Corresponding author: [bsemire@lautech.edu.ng](mailto:bsemire@lautech.edu.ng); ORCID: <https://orcid.org/0000-0002-4173-9165>

Received: 27 December 2024; revised: 15 July 2025; accepted: 08 August 2025

## ABSTRACT

The optoelectronic and charge transfer properties of dyes containing *N,N*-diphenylthiophen-2-amine (NBBT) or *N*-phenyl-*N*-(thiophen-2-yl)-1*H*-pyrrol-2-amine (NTPA) as donor were computationally studied using density functional theory (DFT) and time dependent - density functional theory (TD-DFT) methods. Thiophene, fused thiophene and bridged thiophene derivatives were incorporated to extend the hexatriyne (LCC)  $\pi$ -linker (hexatriyne-thiophene  $\pi$ -linker) to examine the effect thiophene derivatives on the photovoltaic and optoelectronic properties of the designed dyes. The  $\omega$  and  $\omega^+$  values show that insertion of boron into hexatriyne-bridged thiophenes  $\pi$ -linker in NTPA-6 and NBBT-6 dyes trap some of the electrons to be transmitted to the acceptor moiety, which may account for low oscillation strengths observed for the dyes. This subsequently affects the light harvesting efficiency (LHE) and open current circuit (VOC), although, the fractions of electrons transmitted could probably take shorter time ( $\tau_{ns}$ ) getting into the conduction band (CB) of semiconductor. The coupling constant ( $V_{RP}$ ) reveals influence on the rate of regeneration of the dyes. Also, slight lowering of  $E_{HOMO}-E_{LUMO}$  ( $\Delta E_g$ , eV) in respective NTPA dyes than NBBT dyes indicate more electrons are pushed by *N*-phenyl-*N*-(thiophen-2-yl)-1*H*-pyrrol-2-amine into the  $\pi$ -linker than *N,N*-diphenylthiophen-2-amine, and incorporation of fused thiophene and bridged thiophenes (except NTPA-6 and NBBT-6) improve the LHE dyes's ability than PY-3N; thus hexatriyne-thiophene containing dyes exhibit favorable optoelectronic properties, making them good candidates for light absorption in dye sensitized solar cells (DSSCs).

**Keywords:** *N*-phenyl-*N*-(thiophen-2-yl)-1*H*-pyrrol-2-amine, *N,N*-diphenylthiophen-2-amine, hexatriyne-thiophene, DFT, DSSCs

## INTRODUCTION

Dye sensitized solar cell have being one of the reliable, portable and stable sources of electricity energy, in which electricity can be generated through light absorption by a sensitizer. A DSSC contains four main components which are; (i) photoanode through which current enter into the cell by the absorption of light, and it is made up of a non-crystalline metal oxide like titanium oxide, zinc oxide [1], (ii) the photosensitizer which controls light absorption and electron transfer in the DSSC devices. These photosensitizers can be natural and synthetic sensitizers such organic dyes, which have been incorporated as sensitizers over the years,

(iii) the electrolyte which consists of redox coupled with  $I/I_3^-$  [2, 3], and (iv) the cathode through which current leaves the cell [4]. However, dye sensitized solar cells have attracted attention due to low cost of fabrication, large charge separation, separation of the absorption of photons from the energy generation, less contamination and suitable for processing at ambient temperature and good plasticity [5].

This unique mechanism of utilizing a dye to absorb light and facilitate electron transfer makes DSSCs an innovative and promising technology for converting sunlight into electrical energy. There are various aspects of DSSCs that can be extensively explored to

improve the performance of the DSSCs such as the design of efficient dyes, optimization of semiconductor materials, and improvements in overall cell performance [6]. Efforts have been made to improve the efficiency of dye sensitizers for solar energy conversation which is generally determined by the light harvesting efficiency, electron injection efficiency and undesirable charge recombination degree. Low efficiency of dye-sensitizer is due to high level of recombination of free electrons in the oxidized dye molecules which result into limitation of electrons transfer in  $\text{TiO}_2$  [7]. However, this is minimized by counter electrode in DSSC by acting as a positive electrode for collecting electrons and providing catalyst for enhancing charge transfer rate as a reflector for unabsorbed light [8].

In order to overcome high charge recombination in oxidized dye, as well as improving light harvesting efficiency of dye-sensitizers, different types of dyes have been used in Dye sensitized solar cells which include metal-organic dyes such as inorganic ruthenium [9] and other metal (Zn, Co, Ni, Cd, Cu and Fe) based dyes [10, 11]. The power conversion efficiency (PCE) of metal based dye-sensitizers for DSSCs has reached about 14-15%, which is now exceeded that of amorphous silicon-based solar cells, though it is not yet efficient as common silicon based solar cells [12]. Also, metal-free organic dyes which have an advantage due to their structural flexibility, low processing cost, ease of purification, readily accessible, tunable electronic and optical properties, higher extinction coefficients and environmental friendliness [13, 14]. The main setback in the use of metal-free organic dye-sensitizers is the low photo-electric conversion efficiency and dye stability [15]. To overcome these shortcomings, several dyes such as D-A, D- $\pi$ -A, D-A- $\pi$ -A, D- $\pi$ -D- $\pi$ -A, (D- $\pi$ -A)<sub>2</sub>, D-D- $\pi$ -A, D- $\pi$ -A-A and A- $\pi$ -D- $\pi$ -A have been designed to improve charge separation and stability [16].

To enhance the electron density of dye-sensitizers, a diverse array of natural dyes such as carotenoids, chlorophylls, beta-carotene, and anthocyanins [17,18] and synthetic organic dyes-including quinoxaline, indoloquinoxaline, coumarin, triphenylamine derivatives, benzothieno-pyrrole, indoline, benzothiadiazole, carbazole, diketopyrrolopyrrole, phenoxazine, phenothiazine, and phthalocyanine have been employed as donor moieties in DSSC designs [19-21]. For anchoring to metal oxides like  $\text{TiO}_2$ , acceptors such as rhodamine-3-acetic acid, cyano-2-pyran-4-ylidene-acetic acid [20, 22, 23], acetylacetonate [24], and bipolar diketopyrrolopyrrole [25] have been explored, though cyanoprop-2-enoic acid remains the most widely used anchoring group due to its electron-withdrawing enhancements [26]. To optimize charge separation,  $\pi$ -linkers such as silole, selenophene [14], thiophene [27], thiophene-fused bridges [28], furan [29, 30], and carbon-bridged bithiophene [29-32], have been tailored to relay

electrons between donor and acceptor units. Notably, linear carbon chain (LCC) linkers, computationally have been studied for their high conductivity and unique optoelectronic behavior [33], have been integrated into dyes featuring pyrrole/thiophene donors and cyanoacrylic acid acceptors, with findings showing that LCCs significantly influence photo-absorption and electrochemical properties [34]. However, extending LCC lengths beyond hexatriyne minimally impacts band gaps while increasing structural distortion, potentially hindering electron transfer rates from donor to acceptor and thus affecting photovoltaic performance [35]. Therefore, in this work, (2E)-2- cyano-3-(5-{6-[5-(1H-pyrrol-2-ylamino)thiophen-2-yl]hexa-1,3,5-triyn-1-yl} thiophen-3-yl)prop-2-enoic acid (Py-3N) dye-sensitizer was used as reference dye, in which N-(thiophen-2-yl)-1H-pyrrol-2-amine donor group [35] was replaced with N,N-diphenylthiophen-2-amine (NBBT) or N-phenyl-N-(thiophen-2-yl)-1H-pyrrol-2-amine (NTPA) donor group. Also, fused thiophene and bridged thiophene derivatives are incorporated to extend the LCC  $\pi$ -linker as shown in Fig. 1, in order to understand the effect thiophene derivatives on the photovoltaic and optoelectronic properties of the designed dyes.

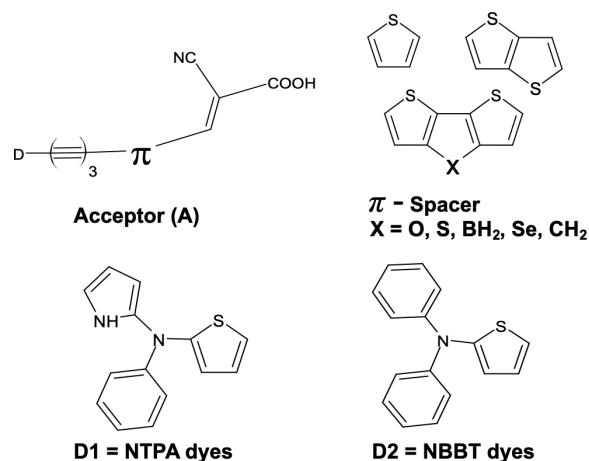


Fig.1. Architectural design of the proposed dye sensitizers containing N-phenyl-N-(thiophen-2-yl)-1H-pyrrol-2-amine (NTPA)/N,N-diphenylthiophen-2-amine (NBBT) donor with hexatriyne-thiophene linkers

## COMPUTATIONAL AND THEORETICAL METHODS

All molecular calculations in this study were refined and executed using the Spartan'14 quantum chemistry software suite for molecular modeling, structural visualizations and graphical analysis of molecular properties [36]. The geometrical optimization of the developed D- $\pi$ -A dyes included the Lee, Yang, and Parr correlation functional along with Becke's gradient exchange correction, employing the 6-31G\*\* basis set at the DFT level of three-parameter density functional (B3LYP). Frequency computations on the geometry were performed at the same theoretical

level to ascertain the local minimum on the potential energy surface. To determine the ultraviolet-visible (UV-vis) absorption spectra of the dyes, the DT-DFT approach was also utilized. This technique has been sufficiently demonstrated to be effective and productive for assessing the excitation properties of organic dyes. The optimized geometries were used to analyze the electrostatic interactions between molecules by computing the molecular electrostatic potential (MEP), the lowest unoccupied molecular orbital (LUMO), and the highest occupied molecular orbital (HOMO) [27, 28, 30].

The energies of the related frontier orbitals at the DFT/6-31G\*\* theoretical level were employed to calculate chemical reactivity parameters such as chemical hardness ( $\eta$ ), chemical potential ( $\mu$ ), global electrophilicity ( $\omega$ ), electron-donating ability ( $\omega^-$ ), and electron-accepting ability ( $\omega^+$ ). Additionally, TD-DFT with the B3LYP functional and the 6-31G\*\* basis set was utilized to obtain the absorption wavelength, oscillator strength, excitation energy, and electronic transitions of all systems without the inclusion of any solvent. It was suggested that this method would suffice for determining the optical and electrical properties of metal-free organic dyes. By evaluating light harvesting efficiency (LHE), open circuit voltage (VOC), electron injection, electron regeneration, and excited state lifetime from the optimized dyes, the photovoltaic characteristics of these molecules were explored. The maximum oscillator strength,  $f$ , was applied to calculate LHE [26,37]. All the dyes were designed and optimized on a system with an Intel(R) Core (TM) i7-8565U CPU operating at 1.80GHz and 1.99 GHz.

$$\text{Chemical hardness } (\eta) = -\frac{(E_{\text{HOMO}} - E_{\text{LUMO}})}{2} = \frac{I - A}{2} \quad (1)$$

$$\text{Chemical potential } (\mu) = \frac{E_{\text{HOMO}} + E_{\text{LUMO}}}{2} = -\frac{(I + A)}{2} \quad (2)$$

$$\text{Global electrophilicity } (\omega) = \frac{\mu^2}{2\eta} = \frac{(I + A)^2}{4(I - A)} \quad (3)$$

$$\text{Electron donating power } (\omega^-) = \frac{(3I - A)^2}{16(I - A)} \quad (4)$$

$$\text{Electron accepting power } (\omega^+) = \frac{(I + 3A)^2}{16(I - A)} \quad (5)$$

where ionization potential (I) and electron affinity (A) are approximated to be negative of the HOMO ( $I = -E_{\text{HOMO}}$ ) and LUMO ( $A = -E_{\text{LUMO}}$ ), respectively. Furthermore, absorption wavelength, oscillator strength, excitation energy, electronic transitions and light harvesting efficiency (LHE) were calculated using TD-DFT with B3LYP/6-31G\*\* basis set. The LHE of the dyes is determined from the absorption coefficient (A), relates to the oscillator strength (f) of the excited state of the maximum wavelength (max) as follows:

$$\text{LHE} = 1 - 10^{-A} \approx 1 - 10^{-f} \quad (6)$$

For the majority of photons to absorb in the UV-Visible region by a dye-sensitizer, and then inject photo excited electrons, the LHE value must be near to unity. The open circuit current (VOC) estimated from the  $E_{\text{LUMO}}$  of the dye and the conduction band ( $E_{\text{CB}}$ ) of the semiconductor ( $\text{TiO}_2$ ) is given in equation 7, and is related to ability of a dye to inject electrons from the excited dye to the conduction band semiconductor. It is taken to be -4.0 eV at pH of 7.0 [26].

$$\text{VOC} = E_{\text{LUMO}} - E_{\text{CB}}^{\text{TiO}_2} \quad (7)$$

The free energy change electron injection ( $\Delta G^{\text{inject}}$ ) for a dye-sensitizer is calculated using the oxidation potential of an excited  $E_{\text{ox}}^{\text{dye*}}$  dye and the conduction band semiconductor, equation 8.

$$\Delta G^{\text{inject}} = E_{\text{ox}}^{\text{dye*}} - E_{\text{CB}}^{\text{TiO}_2} \quad (8)$$

where  $E_{\text{ox}}^{\text{dye*}}$  is the difference between the oxidation potential of the dye in its ground state ( $E_{\text{ox}}^{\text{dye}}$ ) and the electronic vertical transition energy corresponding to  $\lambda_{\text{max}}$  ( $\lambda_{\text{max}}^{\text{ICT}}$ ).

$$E_{\text{ox}}^{\text{dye*}} = E_{\text{ox}}^{\text{dye}} - \lambda_{\text{max}}^{\text{ICT}} \quad (9)$$

The  $\Delta G^{\text{inject}}$  tells about the dye's sensitivity to sunlight absorption which leads to the dye's excitation and subsequent transfer of electrons to the semiconductor  $\text{TiO}_2$ 's conduction band. The regeneration drive force or energy ( $\Delta G^{\text{regen}}$ ), which is calculated using equation 10, is one of the parameters that can affect the performance of DSSCs and its provides information on how charge is recovered in a solar cell system. For fast transfer of electrons,  $\Delta G^{\text{regen}}$  must be very low, but should be around 0.20 eV [26, 38].

$$\Delta G^{\text{regen}} = E_{\text{ox}}^{\text{dye}} - E_{\text{Redox}}^{\text{Electrolyte}} \quad (10)$$

The excited-state lifetime (relays information about the charge transfer characteristics of a material, and it is an appraisal for how fast electrons can get to the semiconductor substrate from the dye or period a photosensitizer stays in excited state before going back to its ground state, therefore, this process must be fast to avert charge recombination [39].

$$\tau_{\text{est}} = \frac{1.499}{fE^2} \quad (11)$$

Another factor that can influence the rate of electron injection into the semiconductor substrate from the dye, is coupling constant, which is estimated using equation 12 [40].

$$|V_{\text{RP}}| = \frac{\Delta E_{\text{RP}}}{2} = [E_{\text{LUMO}}^{\text{dye}} + 2E_{\text{HOMO}}^{\text{dye}}] - [E_{\text{LUMO}}^{\text{dye}} + E_{\text{HOMO}}^{\text{dye}} + E_{\text{CB}}^{\text{TiO}_2}] = \frac{1}{2}(E_{\text{HOMO}}^{\text{dye}} - E_{\text{CB}}^{\text{TiO}_2}) \quad (12)$$

## RESULTS AND DISCUSSION

**The frontier orbital properties:** The optimized structures of the designed dyes at B3LYP/6-31G\*\* level, showing clearly the donor,  $\pi$ -linker and acceptor units are shown in Fig. 2. The frontier orbital energies ( $E_{\text{HOMO}}$ ,  $E_{\text{LUMO}}$  and  $E_{\text{HOMO}} - E_{\text{LUMO}}$  ( $E_g$ )) have great effect on photo-electronic characteristics of dye-sensitizers for dye-sensitized solar cells (DSSCs).

The HOMO of these dyes is principally localized on the donor unit and spread over the hexatriyne  $\pi$ -linker, whereas the LUMO is spread over the acceptor unit, as well as on the thiophene derivatives used as extended  $\pi$ -linker, indicating possibility of electrons transfer from the donor unit through the  $\pi$ -linker to the acceptor unit in a push-pull manner [30] as shown in Fig. 3.

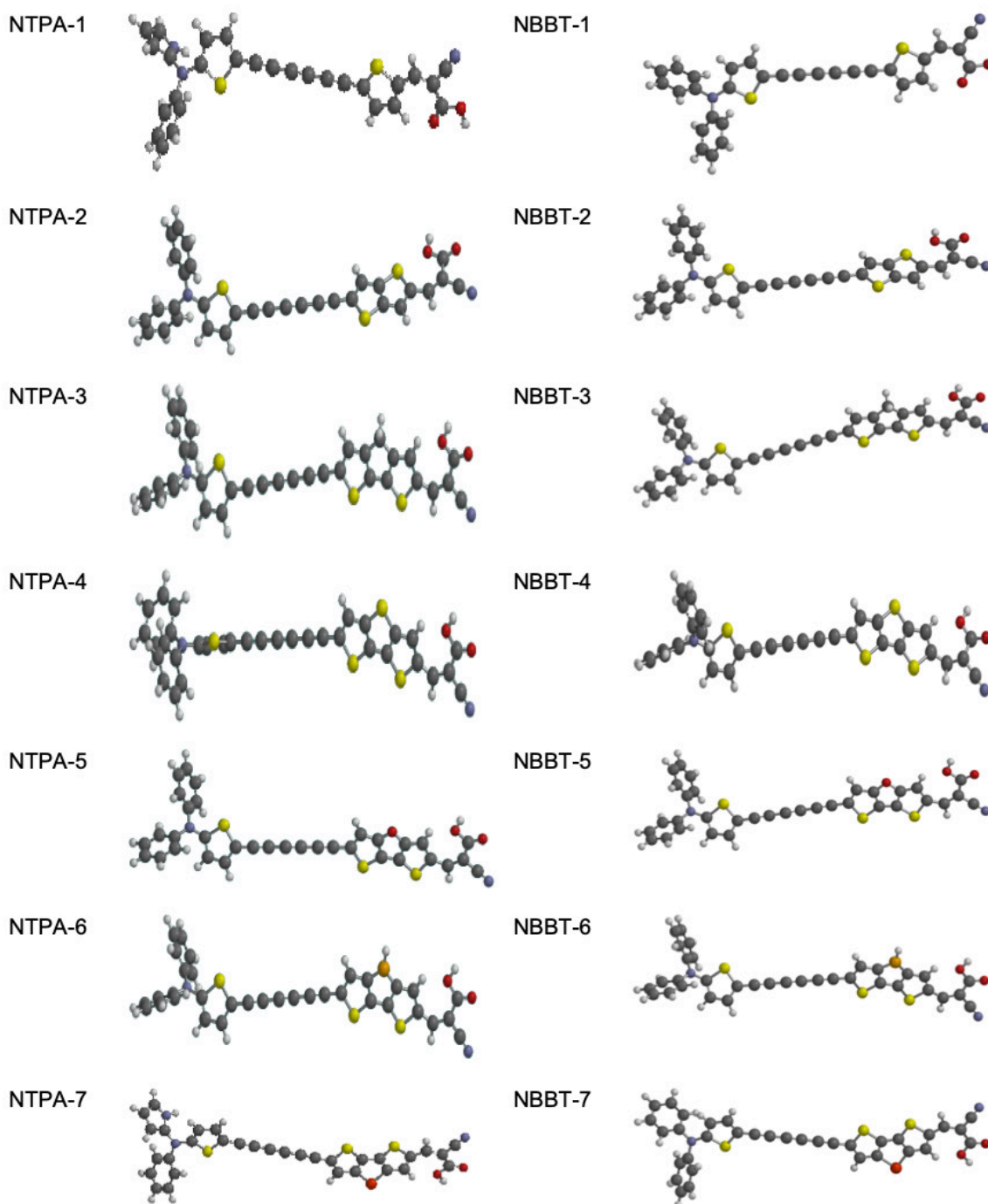


Fig. 2. Frontier orbitals diagram for the studied D-  $\pi$ -A dyes of NTPA and NBBT



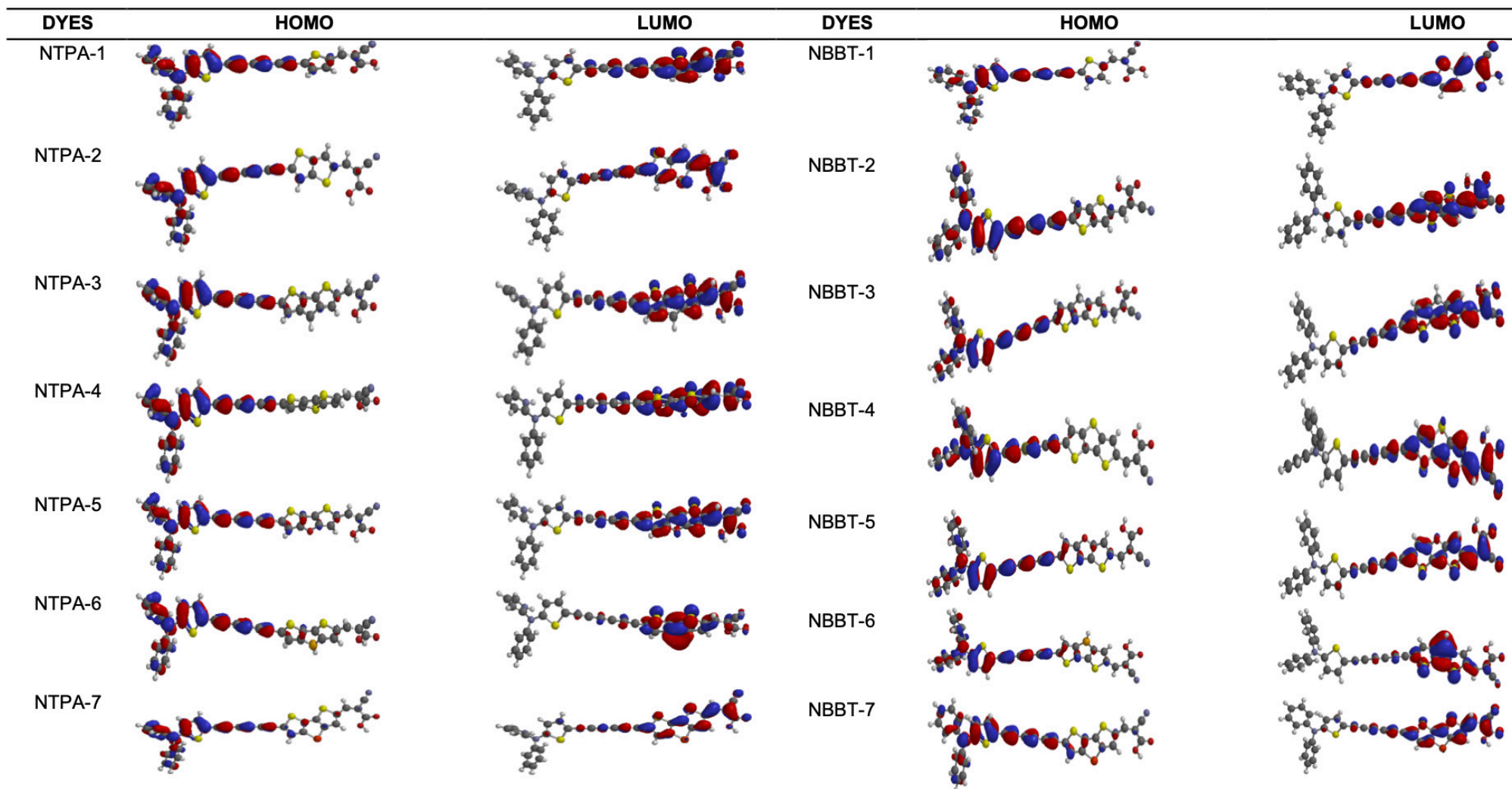


Fig. 3. Frontier orbitals (HOMO and LUMO) overlay

The higher HOMO energy is associated to higher oxidation potential and subsequently higher driving force [40].

The HOMO energy of a dye-sensitizer must be less than that of the electrolyte ( $I/I_3$ ) redox potential (-4.70 eV) for possible regeneration the oxidized sensitizer.

The LUMO energy must be higher than the conduction band (CB, -4.0 eV) of  $\text{TiO}_2$  for the electronic injection to be made possible [40]. The calculated frontier energies (HOMO, LUMO, Eg) for NTPA (1-7) dyes are (-5.15, -3.02, 2.13 eV), (-5.13, -3.03, 2.10 eV), (-5.08, -2.99, 2.09 eV), (-5.13, -3.08, 2.05 eV), -5.12, -3.06, 2.06 eV), (-5.12, -3.44, 1.68 eV), and (-5.08, -3.05, 2.03 eV), respectively. For NBBT (1-7) dyes, the (HOMO, LUMO and Eg) energies are (-5.17, -3.00, 2.17 eV), (-5.19, -3.04, 2.15 eV), (-5.11, -2.98, 2.13 eV), (-5.18, -3.07, 2.11 eV), (-5.15, -3.06, 2.09 eV), (-5.15, -3.44, 1.71 eV) and (-5.14, -3.05, 2.09 eV), respectively (Fig. 4). The HOMO energies of the dyes are less than that of ( $I/I_3$ ), indicating ease of regeneration of the dyes, and also, the LUMO energies of all the dyes are well above the CB (-4.0 eV) of  $\text{TiO}_2$ , which indicate that electrons can be quickly injected into the semiconductor during excitation [17]. However, NBBT dyes have lower HOMO energies than respective NTPA dyes, which mean NBBT dyes could have higher regeneration force than NTPA dyes. Also, *N*-phenyl-*N*-(thiophen-2-yl)-1*H*-pyrrol-2-amine donor in NTPA dyes stabilizes the HOMO energy then *N,N*-diphenylthiophen-2-amine in NBBT dyes which results in slightly lower of Eg in NTPA dyes (Fig. 4). The HOMO, LUMO and Eg values for PY-3N are -5.23, -2.99 and 2.44 eV, respectively, indicating that replacement of *N*-(thiophen-2-yl)-1*H*-pyrrol-2-amine with *N*-phenyl-*N*-(thiophen-2-yl)-1*H*-pyrrol-2-amine (NTPA) and *N,N*-diphenylthiophen-2-amine (NBBT) destabilized both the HOMO and LUMO leading lower Eg; this may lead to shift in absorption to longer wavelengths [41]. The effects of extension of  $\pi$ -linker with thiophene derivatives reveal that when thiophene (NTPA-1 and NBBT-1), is replaced with thieno[3,2-*b*]thiophene (NTPA-2 and NBBT-2), the HOMO is stabilized by 0.2 eV in both NTPA and NBBT dyes resulting to lowering of Eg by 0.30 and 0.20 eV in NTPA and NBBT dyes, respectively.

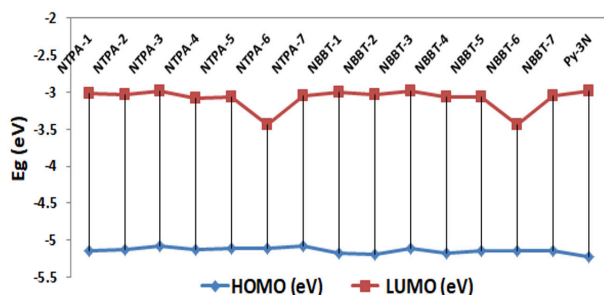


Fig. 4. The Frontier orbital energies of NTPA and NBBT dyes

Also, replacing thiophene with 4*H*-cyclopenta[1,2-*b*:5,4-*b'*]bisthiophene ( $X = \text{CH}_2$ ) as represented by NTPA-3 and NBBT-3) shows that the HOMO is stabilized by 0.70 eV and subsequent reduction of Eg by 0.40 eV in both NTPA-3 and NBBT-3 dyes.

Furthermore, exchanging  $X = \text{CH}_2$  with S, O, B and Se leads to destabilization of both the HOMO and LUMO energies in both NTPA (4-7) and NBBT (4-7), which result in lowering of Eg compare to NTPA-3. This effect is much noticeable in NTPA-6 and NBBT-6 dyes where the LUMO energies is strongly destabilized and results in additional reduction of Eg (1.68 and 1.71 eV for NTPA-6 and NBBT-6, respectively).

**Molecular electrostatic potential:** The molecular electrostatic potential (MEP) properties of the dye-sensitizers simulated at B3LYP/6-31G\*\* are displayed in Fig. 5. MEP provides information about the distribution of electron density on the molecular surface, and also gives information on charge forms, densities, delocalization and transfer processes in molecules. It is also provide essential information on the reactive sites and centre for hydrogen bonding [23]. The MEP map exhibits range of colours from red (negative charge/potential) → orange (less negative charge/potential) → green (less positive charge/potential) → blue (positive charge/potential). The red region represents the high electron density area or negative electrostatic potential region and the blue region is a low electron density area or positive electrostatic potential region. The green region is an intermediate region [22, 40]. The prominent blue colour (acidic arena) is on hydroxyl hydrogen atom of carboxylic acid signifying electrophilic centre, i.e. the hydroxyl hydrogen can be easily given away to pave way for effective coupling/anchoring with  $\text{TiO}_2$  [42]. The red colour is prominently on carbonyl oxygen of carboxylic group and cyano group, signifying nucleophilic centre high profitable sites for the electrolyte [40]. Thus all designed dyes can anchoring with  $\text{TiO}_2$  and also interact with electrolyte effectively.

**Reactivity indicators:** The reactivity indices calculated for the dyes are ionization potential ( $\text{IP} = -E_{\text{HOMO}}$ ), electron affinity ( $\text{EA} = -E_{\text{LUMO}}$ ), chemical hardness ( $\eta$ ), electrophilicity index ( $\omega$ ), electron-donating power ( $\omega^-$ ) and electron-accepting power ( $\omega^+$ ) as listed in Table 1. The IP and EA are linked to energies change in molecule when holes are created or electrons are extracted and when electrons are absorbed or holes are extracted, respectively. The ability to create holes by injecting excited electron into  $\text{TiO}_2$  go gaining electrons from the electrolyte ( $I/I_3$ ) to fill the holes are essential qualities a dye must possess to function as dye-sensitizer in DSSCs [30]. The IP for NTPA (1-7) are well favoured that the respective NBBT (1-7), but EA values favour NTPA-6 and NBBT-6 (Table 1). The chemical hardness,  $\eta$  (inverse of Eg) is related to the ease of charge transfer within a molecule/dye.

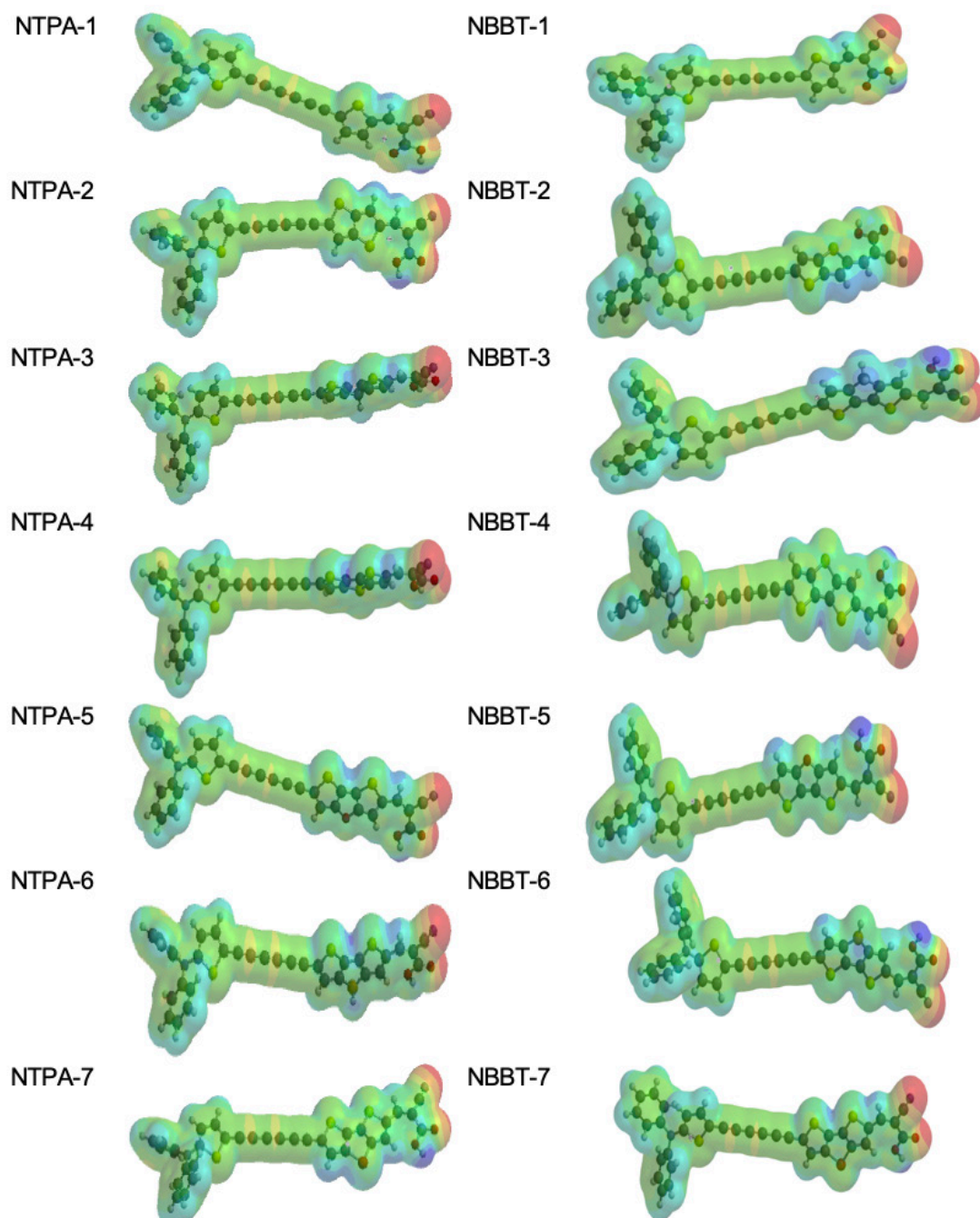


Fig. 5. Molecular Electrostatic Potential of NTPA and NBBT

The lower value of  $\eta$  enhances intramolecular charge transfer and separation [28]; thus the  $\eta$  values of the dyes can be ordered as: NTPA-6 < NTPA-7 < NTPA-4, NTPA-5, NTPA-3 < NTPA-2 < NTPA-1, and NBBT-6 < NBBT-5, NBBT-7 < NBBT-4 < NBBT-3 < NBBT-2 < NBBT-1 < PY-3N.

This shows that NTPA and NBBT dyes should be favoured for intramolecular charge transfer and separation and thus may enhance light to energy conversion efficiency in DSSC than PY-3N.

Among the NTPA and NBBT dyes, NTPA-6 and NBBT-6 will be most favoured for enhance intramolecular charge transfer and separation [27]. The stabilization energy and electron-accepting ability of a dye are measured by  $\omega$  and  $\omega^+$ , respectively, the higher values of  $\omega$  and  $\omega^+$  are desirable for a dye to be used as a sensitizer [27]. The  $\omega$  and  $\omega^+$  can be arranged as NTPA-6/NBBT-6 > NTPA-4/NBBT-4 > NTPA-5/NBBT-5 > NTPA-7/NBBT-7 > NTPA-2/NBBT-2 > NTPA-1/NBBT-1 > NTPA-3/NBBT-3, indicating that NTPA-6

Table 1. Reactivity properties of the designed dyes (NTPA and NBBT)

Dye	IP (eV)	EA (eV)	$\eta$ (eV)	$\mu$ (eV)	$\omega$ (eV)	$\omega^-$ (eV)	$\omega^+$ (eV)
PY-3N	5.23	2.99	1.12	-4.11	7.541	4.500	6.166
NTPA-1	5.15	3.02	1.06	-4.09	7.834	4.534	6.189
NTPA-2	5.13	3.03	1.05	-4.08	7.927	4.547	6.201
NTPA-3	5.08	2.99	1.04	-4.04	7.790	4.488	6.123
NTPA-4	5.13	3.08	1.03	-4.11	8.222	4.620	6.288
NTPA-5	5.12	3.06	1.03	-4.09	8.120	4.590	6.251
NTPA-6	5.12	3.44	0.84	-4.28	10.903	5.286	7.116
NTPA-7	5.08	3.05	1.01	-4.07	8.140	4.575	6.226
NBBT-1	5.17	3.00	1.09	-4.09	7.690	4.507	6.163
NBBT-2	5.19	3.04	1.08	-4.12	7.876	4.564	6.232
NBBT-3	5.11	2.98	1.07	-4.05	7.682	4.475	6.115
NBBT-4	5.18	3.07	1.06	-4.13	8.064	4.606	6.279
NBBT-5	5.15	3.06	1.05	-4.11	8.062	4.591	6.256
NBBT-6	5.15	3.44	0.86	-4.30	10.788	5.272	7.100
NBBT-7	5.14	3.05	1.05	-4.10	8.034	4.576	6.237

and NBBT-6 are most probable for electron-accepting power and stabilization abilities, as well as electrophilic and electron accepting power (Table 1), thus trap some of the electrons which may lead to lower probability electron transmitting (lower oscillation strength) to the acceptor moiety.

**The electronic absorption of the dyes:** The essential information on the electronic transitions of a molecule can be obtained by probing the molecular orbitals accompanying each electronic transition. Tables 2 and 3 contain absorption peaks, oscillation strength and molecular orbitals involved in transitions as calculated at B3LYP/6-31G\*\* for NTPA and NBBT dyes. Since photo-current conversion relies primarily on absorption in the visible and near-ultra violet (UV) regions of the spectrum, the absorption wavelengths longer than 300 nm for singlet-singlet transitions, transition oscillation intensity ( $f > 0.2$ ) and molecular orbitals involve in the transitions of the dyes are listed in Table 2. The absorption  $\lambda_{\max}$  and longest wavelength in nm are 438.88 and 640.03 for NTPA-1, 460.05 and 621.11 for NTPA-2, 477.56 and 667.69 for NTPA-3, 471.50 and 691.37 for NTPA-4, 431.96 and 649.82 for NTPA-5, 538.88 and 861.46 for NTPA-6, 471.99 and 630.85 for NTPA-7 (Table 2). For NBBT dyes, the  $\lambda_{\max}$  and longest wavelength in nm is 595.65 for NBBT-1, 450.9 and 637.52 for NBBT-2, 474.59 and 640.41 for NBBT-3, 468.79 and 673.74 for NBBT-4, 471.55 and 637.45 for NBBT-5, 530.12 and 841.66 for NBBT-6, 630.85 and 630.85 for NBBT-7 (Table 3). However, PY-3N dye presents two absorption peaks at 432.91 and 577.39 nm indicating that NTPA and NBBT dyes experience bathochromic or red shift which may lead to increase in charge transfer to  $\text{TiO}_2$  and photo-excitation [27]. The longest wavelength of all the dyes arises from HOMO→LUMO orbital contributions indicating  $\pi \rightarrow \pi^*$  transitions.

The NTPA-6 and NBBT-6 display highest  $\lambda_{\max}$  and longest wavelength with lowest oscillation strengths of 0.4870 and 0.3531 for NTPA-6, and 0.7318 and 0.4553 for NBBT-6, respectively. The lower electron transition probability in both NTPA-6 and NBBT-6 as reflected by oscillation strengths may lead to low light harvesting efficiency (LHE) and open current circuit (VOC); however, the mobility of fractions of transited electrons in both NTPA-6 and NBBT-6 are higher than the other dyes resulting into longer wavelengths.

**Dipole moment, polarizability and hyperpolarizability:** The static polarizability ( $\alpha$ ), hyperpolarizability ( $\beta$ ) and electric dipole moment ( $\mu$ ) based on the finite field method were calculated for the dyes at DFT B3LYP/6-31G\*\*. The total static dipole moment ( $\mu$ ), mean polarizability ( $\alpha$ ) and mean first hyperpolarizability ( $\beta$ ) are defined by using the x,y,z component, as shown in equations (17) to (22):

$$\mu_{\text{Total}} = (\mu_x^2 + \mu_y^2 + \mu_z^2)^{1/2} \quad (17)$$

$$\alpha_0 = 1/3 (\alpha_{xx} + \alpha_{yy} + \alpha_{zz}) \quad (18)$$

$$\beta_0 = \beta_{\text{Total}} = (\beta_x^2 + \beta_y^2 + \beta_z^2)^{1/2} \quad (19)$$

$$\beta_x^2 = (\beta_{xxx} + \beta_{xyy} + \beta_{xzz})^2 \quad (20)$$

$$\beta_y^2 = (\beta_{yyy} + \beta_{yzz} + \beta_{yxx})^2 \quad (21)$$

$$\beta_z^2 = (\beta_{zzz} + \beta_{zxx} + \beta_{zyy})^2 \quad (22)$$

Non-linear optical (NLO) properties is also a useful parameter to evaluate sensitivity of a molecule to photon absorption and harmonic production, as well as charge delocalization and intramolecular charge transfer; this has connection with dipole moment, polarizability and hyperpolarizability values of a molecule [43].



Table 2. Calculated absorption peaks, oscillation strength and molecular orbitals involved in transition calculated for NTPA (1-7) dyes at TD-DFT B3LYP/6-31G\*\*

Dye	$\lambda$ nm	E eV	f	MO interactions
PY-3N	352.30	3.52	0.2756	H-1 $\rightarrow$ L+1(0.73)
	423.91	2.93	1.2254	H-1 $\rightarrow$ L(0.42), H $\rightarrow$ L+1(0.11), H $\rightarrow$ L+2 (0.30),
	435.70	2.85	0.1733	H-2 $\rightarrow$ L(0.84)
	490.90	2.53	0.1086	H $\rightarrow$ L+1(0.67), H $\rightarrow$ L+2(0.25)
	577.39	2.15	1.2078	H $\rightarrow$ L(0.91)
NTPA-1	376.78	3.29	0.3856	H-1 $\rightarrow$ L+1(0.78)
	402.86	3.07	0.0250	H $\rightarrow$ L+2(0.37), H $\rightarrow$ L+1(0.20), H-3 $\rightarrow$ L (0.18), H-1 $\rightarrow$ L (0.14)
	438.88	2.82	1.2279	H-2 $\rightarrow$ L (0.32), H-1 $\rightarrow$ L (0.28), H-3 $\rightarrow$ L (0.12)
	451.41	2.74	0.3007	H-2 $\rightarrow$ L (0.38), H-1 $\rightarrow$ L (0.36), H $\rightarrow$ L+1(0.11)
	475.83	2.60	0.1888	H $\rightarrow$ L+2 (0.42), H $\rightarrow$ L+1(0.40)
	640.03	1.93	0.7746	H $\rightarrow$ L (0.92)
NTPA-2	381.80	3.24	0.0168	H-1 $\rightarrow$ L+1(0.45), H-1 $\rightarrow$ L+2(0.43)
	419.21	2.95	0.0423	H $\rightarrow$ L+1 (0.35), H-2 $\rightarrow$ L (0.24), H-1 $\rightarrow$ L (0.19), H $\rightarrow$ L+2 (0.15)
	426.35	2.91	0.0015	H-3 $\rightarrow$ L (0.86)
	460.05	2.69	1.3858	H-1 $\rightarrow$ L (0.61), H $\rightarrow$ L+1(0.19) H $\rightarrow$ L+2 (0.11)
	511.39	2.42	0.0328	H $\rightarrow$ L+2 (0.61), H $\rightarrow$ L+1(0.30),
	621.11	1.99	1.3755	H $\rightarrow$ L (0.96)
NTPA-3	399.74	3.10	0.3335	H-1 $\rightarrow$ L+2(0.44), H-1 $\rightarrow$ L+1(0.38)
	438.25	2.83	0.2722	H-2 $\rightarrow$ L (0.62), H-3 $\rightarrow$ L (0.18)
	443.38	2.79	0.0038	H $\rightarrow$ L+1(0.50), H-1 $\rightarrow$ L (0.28)
	477.56	2.59	2.2877	H-1 $\rightarrow$ L (0.52), H $\rightarrow$ L+1(0.31)
	667.69	1.85	0.7591	H $\rightarrow$ L (0.95)
NTPA-4	414.13	3.03	0.3085	H-1 $\rightarrow$ L+1 (0.53), H-1 $\rightarrow$ L+2 (0.27)
	443.71	2.84	0.0355	H $\rightarrow$ L+1 (0.5), H-2 $\rightarrow$ L (0.21), H-1 $\rightarrow$ L (0.16)
	446.51	2.80	0.0675	H-2 $\rightarrow$ L (0.54), H $\rightarrow$ L+2 (0.13)
	471.50	2.59	2.7305	H-1 $\rightarrow$ L (0.47), H $\rightarrow$ L+2 (0.32)
	484.33	2.57	0.3259	H $\rightarrow$ L+2 (0.39), H-1 $\rightarrow$ L (0.20), H $\rightarrow$ L+1 (0.18), H-2 $\rightarrow$ L (0.11)
	691.37	1.87	0.2865	H $\rightarrow$ L (0.95)
NTPA-5	395.22	3.13	0.3936	H-1 $\rightarrow$ L+2(0.59), H-1 $\rightarrow$ L+1(0.23)
	431.96	2.87	0.2175	H-3 $\rightarrow$ L (0.45), H-2 $\rightarrow$ L (0.30)
	437.28	2.83	0.0021	H $\rightarrow$ L+1(0.40), H-2 $\rightarrow$ L (0.32), H-1 $\rightarrow$ L (0.22)
	476.93	2.60	2.0829	H-1 $\rightarrow$ L (0.54), H $\rightarrow$ L+1 (0.38)
	503.94	2.46	0.0697	H $\rightarrow$ L+2(0.87)
	649.82	1.90	1.1298	H $\rightarrow$ L (0.94)
NTPA-6	462.20	2.68	0.0587	H-3 $\rightarrow$ L (0.71)
	478.74	2.59	0.4108	H $\rightarrow$ L+3(0.71)
	510.34	2.43	0.0588	H-2 $\rightarrow$ L (0.84)
	538.88	2.30	0.4870	H $\rightarrow$ L+1(0.76)
	677.80	1.83	0.1454	H-1 $\rightarrow$ L (0.83)
	861.46	1.44	0.3531	H $\rightarrow$ L (0.97)
NTPA-7	398.13	3.11	0.0494	H-3 $\rightarrow$ L (0.95)
	442.19	2.80	0.0080	H $\rightarrow$ L+1(0.45), H-1 $\rightarrow$ L (0.30), H-2 $\rightarrow$ L (0.19)
	480.50	2.58	1.7739	H-1 $\rightarrow$ L (0.55), H $\rightarrow$ L+1(0.36)
	516.42	2.40	0.0323	H $\rightarrow$ L+2(0.87)
	646.68	1.91	1.3426	H $\rightarrow$ L (0.97)

Table 3. Calculated absorption peaks, oscillation strength and molecular orbitals involved in transition calculated for NBBT (1-7) dyes at TD-DFT B3LYP/6-31G\*\*

Dye	$\lambda$ nm	E eV	f	MO interactions
NBBT-1	359.92	3.44	0.0045	H-1 $\rightarrow$ L+1 (0.49), H-1 $\rightarrow$ L+2 (0.42)
	385.16	3.22	0.0275	H-1 $\rightarrow$ L (0.25), H $\rightarrow$ L+1 (0.24), H-3 $\rightarrow$ L (0.24), H $\rightarrow$ L+2 (0.21)
	437.55	2.83	0.8294	H-1 $\rightarrow$ L (0.44), H $\rightarrow$ L+2 (0.19), H-2 $\rightarrow$ L (0.14), H $\rightarrow$ L+1 (0.14)
	438.27	2.83	0.1828	H-2 $\rightarrow$ L (0.80)
	595.65	2.08	1.5267	H $\rightarrow$ L (0.95)
NBBT- 2	384.74	3.22	0.6984	H-1 $\rightarrow$ L+1 (0.67) , H-1 $\rightarrow$ L+2 (0.15)
	404.83	3.06	0.0423	H-1 $\rightarrow$ L (0.25) , H $\rightarrow$ L+1 (0.24), H-2 $\rightarrow$ L (0.19), H $\rightarrow$ L+2 (0.18)
	430.94	2.88	0.0772	H-2 $\rightarrow$ L (0.66)
	450.90	2.75	1.7878	H-1 $\rightarrow$ L (0.53), H $\rightarrow$ L+1 (0.27)
	478.79	2.59	0.3280	H $\rightarrow$ L+2 (0.63), H $\rightarrow$ L+1 (0.23)
	637.52	1.94	0.8605	H $\rightarrow$ L (0.93)
NBBT- 3	398.89	3.11	0.6914	H-1 $\rightarrow$ L+1 (0.39), H-1 $\rightarrow$ L+2 (0.34)
	419.43	2.96	0.0072	H-2 $\rightarrow$ L (0.59)
	436.88	2.84	0.0835	H $\rightarrow$ L+1 (0.35), H-3 $\rightarrow$ L (0.28), H-1 $\rightarrow$ L (0.13),
	474.59	2.61	1.8437	H-1 $\rightarrow$ L (0.58), H $\rightarrow$ L+1 (0.23), H $\rightarrow$ L+2 (0.11)
	485.69	2.55	0.7018	H $\rightarrow$ L+2 (0.73)
	640.41	1.94	0.9913	H $\rightarrow$ L (0. 92)
NBBT- 4	409.77	3.03	0.5666	H-1 $\rightarrow$ L+1 (0.48), H-1 $\rightarrow$ L+2 (0.18), H $\rightarrow$ L+1 (0.13)
	421.82	2.94	0.0034	H-2 $\rightarrow$ L (0.68)
	442.36	2.80	0.0236	H $\rightarrow$ L+1 (0.45), H-1 $\rightarrow$ L (0.12)
	468.79	2.64	2.2357	H $\rightarrow$ L+2 (0.43), H-1 $\rightarrow$ L (0.39)
	473.36	2.62	0.8968	H $\rightarrow$ L+2 (0.33), H-1 $\rightarrow$ L (0.33), H $\rightarrow$ L+1 (0.22)
	673.74	1.84	0.3112	H $\rightarrow$ L (0.94)
NBBT- 5	388.25	3.19	0.5824	H-1 $\rightarrow$ L+2 (0.59), H-1 $\rightarrow$ L+1 (0.21)
	417.92	2.97	0.0049	H-2 $\rightarrow$ L (0.54), H $\rightarrow$ L+1 (0.16) , H-1 $\rightarrow$ L (0.15)
	432.65	2.87	0.1286	H-3 $\rightarrow$ L (0.36), H $\rightarrow$ L+1 (0.23), H-1 $\rightarrow$ L (0.19)
	471.55	2.63	2.0660	H-1 $\rightarrow$ L (0.49), H $\rightarrow$ L+1 (0.44)
	498.94	2.48	0.1262	H $\rightarrow$ L+2 (0.89)
	637.45	1.94	1.2569	H $\rightarrow$ L (0.94)
NBBT-6	459.67	2.70	0.0559	H-3 $\rightarrow$ L (0.60), H-2 $\rightarrow$ L (0.15), H-1 $\rightarrow$ L+1 (0.12)
	478.74	2.59	0.1480	H-2 $\rightarrow$ L (0.48), H $\rightarrow$ L+3 (0.25)
	483.47	2.56	0.3669	H $\rightarrow$ L+3 (0.46), H-2 $\rightarrow$ L (0.25)
	530.12	2.34	0.7318	H $\rightarrow$ L+1 (0.79)
	664.28	1.87	0.0773	H-1 $\rightarrow$ L (0.83)
	841.66	1.47	0.4553	H $\rightarrow$ L (0.95)
NBBT-7	397.80	3.12	0.0681	H-2 $\rightarrow$ L (0.46), H-3 $\rightarrow$ L (0.40)
	423.73	2.93	0.0122	H-4 $\rightarrow$ L (0.45), H-1 $\rightarrow$ L (0.17), H $\rightarrow$ L+1 (0.16), H-3 $\rightarrow$ L (0.12)
	426.09	2.91	0.0114	H-3 $\rightarrow$ L (0.23), H-1 $\rightarrow$ L (0.23), H $\rightarrow$ L+1 (0.21), H-2 $\rightarrow$ L (0.15)
	471.99	2.63	1.7116	H $\rightarrow$ L+1 (0.45), H-1 $\rightarrow$ L (0.44)
	508.96	2.44	0.0330	H $\rightarrow$ L+2 (0.88)
	630.85	1.97	1.5107	H $\rightarrow$ L (0.97)

The dipole moments (Debye) of the designed dyes are NTPA-5 (14.4784) > NTPA-3 (14.0778) > NTPA-2 (13.9592) > NTPA-7 (13.9203) > NTPA-6 (13.8082) > NTPA-4 (13.7892) > PY-3N (11.7918) > NTPA-1 (11.0587) for NTPA dyes (Table 4a), and NBBT-5 (14.4079) > NBBT-7 (14.1271) > NBBT-6 (13.9045) > NBBT-3 (13.7400) > NBBT-1 (10.5897) > NBBT-4 (9.8038) > NBBT-2 (8.8636) for NBBT dyes (Table 4b). This shows that all the dyes (except NTPA-1, NBBT-1, NBBT-2, and NBBT-4) have very high dipole moment than PY-3N, and thus should be able to inject electrons into conduction band (CB) of a semiconductor ( $\text{TiO}_2$ ) in DSSCs than PY-3N. Also, NTPA dyes have higher dipole moments than the respective NBBT dyes, indicating that NTPA dyes should have higher charge injection into the CB of  $\text{TiO}_2$  [43].

The polarizability,  $\alpha$  ( $\times 10^{-23}$  esu) calculated for the dyes are all negative in values, indicating that their excess electron clouds can be easily polarized, which is suitable for electrons injection. The hyperpolarizability,  $\beta$  ( $\times 10^{-30}$  esu) values are arranged as 14.6477, 28.9679, 34.3485, 31.6914, 34.1275, 33.833 and 28.1309 for NTPA (1-7) dyes, and 15.3444, 21.4863, 21.4863, 36.4248, 36.3239, 35.8485 and 30.3885 for NBBT (1-7) dyes, respectively (Tables 4a and 4b). The polarizability and hyperpolarizability for PY-3N are -2.64 and 14.63, respectively, indicating that both NTPA and NBBT dyes are suitable for ICT and electron injection abilities than PY-3N (except NTPA-1) [44], however, NTPA-3, NTPA-4, NTPA-6, NTPA-7 and NBBT-(4-7) have outstanding polarizability and hyperpolarizability properties other studied dyes (Tables 4a and 4b).

Table 4a. Dipole moment, polarizability and hyperpolarizability of NTPA (1-7) dyes

Parameter	PY-3N	NTPA-1	NTPA-2	NTPA-3	NTPA-4	NTPA-5	NTPA-6	NTPA-7
Dipole moment								
$\mu_x$	11.6752	10.5361	13.9227	12.9259	12.9595	14.1556	13.0967	13.1965
$\mu_y$	-1.4033	-1.2382	-0.1595	-1.8104	-1.4911	-1.4711	-0.4799	-3.9372
$\mu_z$	0.8766	3.1231	0.9958	5.2752	4.4687	2.6604	4.3488	2.0313
Total	11.7918	11.0587	13.9592	14.0778	13.7892	14.4784	13.8082	13.9203
Polarizability/a.u								
$\alpha_{xx}$	-180.6957	-247.3459	-354.3533	-373.2709	-355.3051	-371.3299	-363.6722	-346.0301
$\alpha_{xy}$	41.4711	28.3429	1.4209	27.6461	26.9061	25.9077	18.3524	61.7340
$\alpha_{yy}$	-169.2794	-198.3167	-212.8263	-238.0607	-246.1665	-234.3627	-239.0214	-249.8260
$\alpha_{xz}$	-3.313	-19.4660	16.4690	-36.0655	-30.0433	-5.0698	-34.4674	1.2387
$\alpha_{yz}$	3.3092	4.9109	2.6299	-0.6250	1.0256	0.3090	2.6293	3.4157
$\alpha_{zz}$	-185.3804	-205.4578	-228.0718	-237.9752	-248.0283	0.3090	-241.5376	-258.1851
$\alpha_{\text{total}}$	-178.45183	-217.0401	-265.0838	-283.1023	-283.1666	-201.7945	-281.4104	-284.6804
$\alpha \times (10^{-23})$	-2.64	-3.22	-3.928	-4.19	-4.19	-2.99	-4.17	-4.23
Hyperpolarizability								
$\beta_{xxx}$	1614.9671	1403.1924	3273.5456	3776.208	3426.283	3823.008	3652.372	3009.435
$\beta_{xxy}$	-351.9128	-336.7916	58.8733	-260.6649	-280.6100	-288.0669	-154.5772	-743.3114
$\beta_{xyy}$	88.0624	85.7665	22.7515	70.1581	82.1226	50.8835	99.5680	102.4621
$\beta_{yyy}$	-22.2406	-32.5791	-70.8856	-36.0352	-25.6369	-55.9411	-14.7235	-148.4282
$\beta_{xxz}$	185.527	507.8358	31.0776	743.9160	720.0516	375.2337	786.5392	292.2991
$\beta_{xyz}$	16.5627	18.9830	42.5517	68.9239	59.5994	71.3078	41.3621	50.7702
$\beta_{yyz}$	-1.1304	10.2951	4.6117	13.4559	8.4580	15.4237	3.6413	23.8292
$\beta_{zzz}$	-28.4773	69.5315	56.1510	30.8509	65.2456	36.5384	67.5079	-5.7115
$\beta_{yzz}$	-11.5651	-6.3274	-6.7203	-18.0751	16.1847	-10.6029	-4.4820	-19.5649
$\beta_{zzz}$	1.2865	33.9533	30.3780	65.1257	47.4634	43.4633	57.8349	36.5736
$\beta_{\text{total}} \times (10^{-30})$	14.93	14.6477	28.9679	34.3485	31.6914	34.1275	33.8330	28.1309

**Photovoltaic properties:** The photovoltaic properties are vital indicators of the performance of dye-sensitizer in DSSCs and they are peculiar characteristics of a dye. These essential properties are electron injection drive force ( $\Delta G_{\text{inject}}$ ), open-circuit voltage (VOC), electron regeneration drive force ( $\Delta G_{\text{regen}}$ ), light-harvesting efficiency (LHE), ground state oxidation energy of dye ( $E^{\text{dye}}$ ), excited state oxidation energy of dye ( $E^{\text{dye*}}$ ) and the excitation lifetime ( $\tau$ ) as listed in Tables 5 and 6. VOC relates to the ability of the LUMO of a dye to

release electrons into the CB of semiconductor ( $\text{TiO}_2$ ); thus, higher LUMO energy will lead to higher VOC and subsequently higher power conversion efficiency (PCE) of a dye-sensitizer in DSSCs. The calculated VOC values for both NTPA and NBBT dyes are between 0.92 and 1.02 eV, except NTPA-6 and NBBT-6 dyes with 0.56 eV value. The low VOC value for both NTPA-6 and NBBT-6 dyes can be attributed to the low oscillation strengths (Table 5).

Table 4b. Dipole moment, polarizability and hyperpolarizability of NBBT (1-7) dyes

Parameter	NBBT-1	NBBT-2	NBBT-3	NBBT-4	NBBT-5	NBBT-6	NBBT-7
Dipole moment							
$\mu_x$	10.2558	8.6624	12.9671	9.7231	14.2096	13.1259	13.3067
$\mu_y$	-2.0799	1.6788	-2.3287	0.1925	-2.0193	-1.1328	-4.6908
$\mu_z$	1.6229	0.8317	3.9010	-1.2406	1.2633	2.9664	0.7094
Total	10.5897	8.8636	13.7400	9.8038	14.4079	13.9045	14.1271
Polarizability/a.u							
$\alpha_{xx}$	-247.4056	-289.6085	-371.5906	-328.6790	-369.2030	-362.0603	-341.5061
$\alpha_{xy}$	21.7015	-24.1172	21.2225	-0.3998	20.3751	11.6933	55.4849
$\alpha_{yy}$	-200.1883	-226.1014	-239.7521	-249.2652	-235.9048	-240.9837	-252.6576
$\alpha_{xz}$	-28.3916	-15.6466	-48.2485	15.4984	-15.9952	-45.7122	-8.9723
$\alpha_{yz}$	1.1991	-4.5210	-3.3563	-3.6131	-2.5076	-0.6018	-0.7069
$\alpha_{zz}$	-219.4136	-234.2524	-251.7634	-255.4179	-254.3105	-255.1754	-271.4198
$\alpha_{total}$	-222.3358	-249.9874	-287.7020	-277.7874	-286.4728	-286.0731	-288.5278
$\alpha \times (10^{-23})$	-3.29	-3.70	-4.26	-4.11	-4.24	-4.23	-4.27
Hyperpolarizability							
$\beta_{xxx}$	1535.2935	2399.1179	4092.0137	3084.8341	4139.2500	3964.3809	3309.4380
$\beta_{xxy}$	-429.8458	332.8385	-359.9608	57.8961	-391.3726	-258.8486	-876.4440
$\beta_{xyy}$	110.1539	87.2063	103.8885	77.6528	85.4086	127.3472	130.0785
$\beta_{yyy}$	-24.0848	-21.5128	-24.6319	-5.5193	-44.2086	-4.8886	-140.9592
$\beta_{xxz}$	479.2115	160.9916	703.4199	-219.2834	328.4454	745.2589	244.3339
$\beta_{xyz}$	-11.6156	18.8049	1.0512	31.6357	47.6486	7.8291	12.6683
$\beta_{yyz}$	-0.8742	1.3849	6.5837	-17.6623	10.4776	-5.5427	12.5951
$\beta_{xzz}$	-7.4856	-23.8232	-68.6457	-30.5244	-60.8829	-25.8201	-95.7293
$\beta_{yzz}$	-26.6876	15.6026	-36.0682	11.5735	-29.1644	-23.7273	-40.3691
$\beta_{zzz}$	12.4645	-39.7870	42.4496	-23.5680	16.0968	37.0780	14.1904
$\beta_{total} \times (10^{-30})$	15.3444	21.4863	21.4863	36.4248	36.3239	35.8468	30.3883

( $\alpha$ ): 1 a.u = 0.148  $10^{-24}$  esu and for ( $\beta$ ): 1 a.u. = 8.639 $10^{-33}$  esu.

Table 5. Photovoltaic properties of NTPA and NBBT dyes

Dyes	$\lambda_{max}$ (nm)	f	$E_{ox}^{dye}$	$\lambda_{max}^{ICT}$ eV	$E_{ox}^{dye*}$	VOC	LHE	$\Delta G^{inject}$	$\Delta G^{regen}$
PY-3N	423.91	1.2251	5.23	2.93	2.30	1.01	0.9410	-1.69	0.53
NTPA-1	438.88	1.2279	5.15	2.82	2.33	0.98	0.9401	-1.67	0.45
NTPA-2	460.05	1.3858	5.13	2.69	2.44	0.97	0.9589	-1.56	0.43
NTPA-3	477.56	2.2877	5.08	2.59	2.49	1.01	0.9948	-1.51	0.38
NTPA-4	471.50	2.7305	5.13	2.59	2.54	0.92	0.9981	-1.46	0.38
NTPA-5	476.93	2.0829	5.12	2.60	2.52	0.94	0.9917	-1.48	0.42
NTPA-6	538.88	0.4870	5.12	2.30	2.82	0.56	0.6742	-1.18	0.42
NTPA-7	480.50	1.7739	5.08	2.58	2.50	0.95	0.9837	-1.50	0.38
NBBT-1	595.65	1.5267	5.17	2.08	3.09	1.00	0.9702	-0.91	0.47
NBBT-2	450.90	1.7878	5.19	2.75	2.44	0.96	0.9837	-1.56	0.49
NBBT-3	474.59	1.8437	5.11	2.61	2.50	1.02	0.9857	-1.50	0.41
NBBT-4	468.79	2.2357	5.18	2.64	2.54	0.93	0.9942	-1.46	0.48
NBBT-5	471.55	2.0660	5.15	2.63	2.52	0.94	0.9914	-1.48	0.45
NBBT-6	530.12	0.7318	5.15	2.34	2.81	0.56	0.8146	-1.19	0.45
NBBT-7	471.99	1.7116	5.14	2.63	2.51	0.95	0.9857	-1.49	0.44



This means all the dyes (except NTPA-6 and NBBT-6) will have ease of electrons transfer the excited dyes to the CB of  $\text{TiO}_2$ , which will lead to increase in PCE.

The responsiveness or ability of a dye to adsorb sunlight energy which results into dye's excitation is measured by  $\Delta G_{\text{inject}}$ . The  $\Delta G_{\text{inject}}$  values for the dyes are all negative, which make the dyes suitable for electrons injection into the CB of  $\text{TiO}_2$  [14,45]. The regeneration of the dye after photoexcitation and subsequent electrons injection into the CB of  $\text{TiO}_2$  by receiving electrons from the electrolyte ( is very important for the dye continual usage [17]. The regeneration drive force ( $\Delta G_{\text{regen}}$ ) of a good dye-sensitizer must be  $> 0.20$  eV, and that the dyes including PY-3N dye present  $\Delta G_{\text{regen}}$  values higher than 0.2 eV, indicating that the dyes will have good regenerating ability.

The light harvesting efficiency (LHE) measures the amount of light intensity a dye can absorb, therefore it is related to photocurrent reaction in the dye-sensitizer. Higher LHE will lead to higher photocurrent reaction and higher light collecting efficiency [42]. The LHE values for NTPA (1-7) dyes are 0.9401, 0.9589, 0.9948, 0.9981, 0.9917, 0.6742 and 0.9837, respectively, and are 0.9702, 0.9837, 0.9857, 0.9942, 0.9914, 0.8146 and 0.9857 for NBBT (1-7) dyes, respectively (Table 5), revealing that all dyes may have very strong light harvesting efficiency (except NTPA-6 and NBBT-6), although NTPA-3, NTPA-4, NTPA-5, NBBT-4 and NBBT-5 show outstanding LHE values than PY-3N dye (0.9401). Also, incorporation of fused thiophene and bridged thiophenes (except NTPA-6 and NBBT-6) improve the LHE dyes's ability. The excitation lifetime (measures time taken for dye's excited electrons to get into the CB of semiconductor, and it is also a measure of time require for a dye-sensitizer to stay excited before going back to its ground state; thus, it affects both intra- and inter-charge transfer rate of a dye [17, 39, 40]. The calculated  $\tau$  (ns) values for NTPA dyes are arranged as NTPA-6 (8.94)  $>$  NTPA-1 (2.35)  $>$  NTPA-2 (2.29)  $>$  NTPA-7 (1.95)  $>$  NTPA-5 (1.64)  $>$  NTPA-3 (1.50)  $>$  NTPA-4 (1.22), and NBBT-6 (5.76)  $>$  NBBT-1 (3.48)  $>$  NBBT-7 (1.95)  $>$  NBBT-3 (1.83)  $>$  NBBT-2 (1.71)  $>$  NBBT-5 (1.61)  $>$  NBBT-4 (1.47), which mean NTPA-6 and NBBT-6 present highest  $\tau$  values (Table 6), and are likely to have larger charge separation, superior optical stability and charge recombination process delay which are good for better performance DSSCs [27]. The coupling constant ( $|V_{\text{RP}}|$ ) relates to the value of rate constant of transfer of electrons, higher  $V_{\text{RP}}$  values favour electrons injection into CB of  $\text{TiO}_2$  and thus better sensitizers [45,46]. However, Fig.6 shows a strong direct relationship between  $|V_{\text{RP}}|$  and  $\Delta G_{\text{regen}}$  which suggests that dye's regeneration drive force/energy is favoured by higher coupling constant value. Therefore, it is suggested that  $|V_{\text{RP}}|$  may actually influence the rate at which a dye is regenerated rather than for electron injection processes, this observation agrees with the work reported by Semire et al., [27].

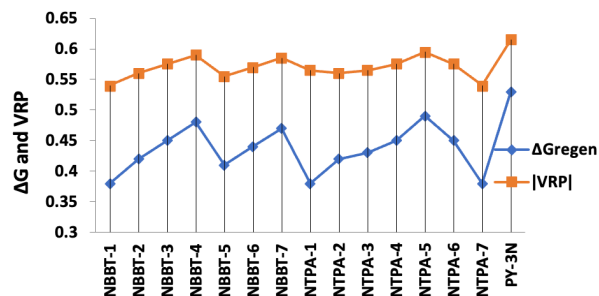


Fig. 6. Influence of coupling constant ( $|V_{\text{RP}}|$ ) on regeneration energy ( $\Delta G_{\text{regen}}$ ) of the dyes

Table 6. Photo excitation response parameters of NTPA and NBBT dyes

Dyes	(ns)	$ V_{\text{RP}} $	LHE	FF
PY-3N	1.37	0.615	0.9410	0.8831
NTPA-1	2.35	0.575	0.9401	0.7343
NTPA-2	2.29	0.565	0.9589	0.7319
NTPA-3	1.50	0.540	0.9948	0.7412
NTPA-4	1.22	0.565	0.9981	0.7191
NTPA-5	1.64	0.560	0.9917	0.7244
NTPA-6	8.94	0.560	0.6742	0.5685
NTPA-7	1.95	0.540	0.9837	0.7269
NBBT-1	3.48	0.585	0.9702	0.7389
NBBT-2	1.71	0.595	0.9837	0.7294
NBBT-3	1.83	0.555	0.9857	0.7435
NBBT-4	1.47	0.590	0.9942	0.7218
NBBT-5	1.61	0.575	0.9914	0.7244
NBBT-6	5.76	0.575	0.8146	0.5685
NBBT-7	1.95	0.570	0.9857	0.7269

LHE = light-harvesting efficiency,  $\tau$ , ns excitation lifetime,  $|V_{\text{RP}}|$  = coupling constant and FF Fill factor

The fill factor (FF), is one of the parameters that FF determine power conversion efficiency (PCE) of a DSSC device, and is strongly affected by VOC of a dye-sensitizer as shown in equation 23 [47,48].

$$FF = \frac{\frac{V_{oc}}{k_b T} - \ln\left(\frac{V_{oc}}{k_b T} + 0.72\right)}{\frac{V_{oc}}{k_b T} + 1} \quad (23)$$

where the Boltzmann constant is  $8.61733034 \times 10^{-5}$  electron volts/K, T is temperature set at 300 K and VOC is open circuit current. NTPA-3 and NBBT-3 have the greatest computed FF values of 0.7412 and 0.7435, respectively, but less than that of PY-3N (0.8831), while both NTPA-6 and NBBT-6 have the least value of 0.5685. This shows that using *N*-phenyl-*N*-(thiophen-2-yl)-1*H*-pyrrol-2-amine and *N,N*-diphenylthiophen-2-amine as donor units couple with extension of LCC  $\pi$ -spacers with thiophene derivatives resulting in a notable modification of the dyes, which is more pronounced in NTPA-6 and NBBT-6 (when X =  $\text{CH}_2$  in 4*H*-cyclopenta[1,2-*b*:5,4-*b'*]bisthiophene is changed to  $\text{BH}_2$ ).

## CONCLUSION

In this work, two set of dyes containing *N,N*-diphenylthiophen-2-amine (NBBT) and *N*-phenyl-*N*-(thiophen-2-yl)-1*H*-pyrrol-2-amine (NTPA) as donors were computationally designed to replace *N*-(thiophen-2-yl)-1*H*-pyrrol-2-amine donor group in PY-3N and optimized using DFT method. Thiophene, fused thiophene and bridged thiophene derivatives were incorporated to extend the hexatriyne (LCC)  $\pi$ -linker in order to examine the effect thiophene derivatives on the photovoltaic and optoelectronic properties of the designed dyes. The results show  $|V_{RP}|$  values may influence the rate of regeneration of the dyes more than that of electron injection processes. The  $\omega$  and  $\omega^*$  show that NTPA-6 and NBBT-6 are more electron accepting abilities than other dyes, thus insertion of boron atom into bridged thiophene trap some of the electrons to be transmitted to the acceptor moiety which leads to lower oscillation strength. Subsequently, it affects light harvesting efficiency (LHE) and open current circuit (VOC), although, the fractions of electrons transmitted could probably take shorter time ( $\tau_{ns}$ ) get into the CB of semiconductor. The polarizability and hyperpolarizability values show that both NTPA and NBBT dyes are suitable for ICT and electron injection abilities, however, NTPA-3, NTPA-4, NTPA-6, NTPA-7, NBBT-4, NBBT-5, NBBT-6 and NBBT-7 have outstanding non-linear properties than PY-3N dye. In general all the designed dyes are capable to transmit electrons through push-pull mechanism to the acceptor unit, thus can serve as dye-sensitizers in DSSCs, and extension of hexatriyne (LCC)  $\pi$ -linker with thiophene derivatives actually modified the dyes.

## FUNDING

This research did not receive any financial support/ grant/fund from any agencies in the public, commercial, or not-for-profit sectors.

## AVAILABILITY OF DATA AND MATERIALS

No data supporting the findings of this study are available in the supporting information of this article.

## DECLARATIONS CONFLICT OF INTEREST

The authors declare no conflict of interest.

## ETHICAL APPROVAL

Not applicable.

## REFERENCES

- Yen Y.S., Chou H.H., Chen Y.C., Hsu C.Y., Lin J.T. (2012) Recent developments in molecule-based organic materials for dye-sensitized solar cells. *J. Mater. Chem.*, **22**, 8734-8747, <https://doi.org/10.1039/C2JM30362K>
- Birel O., Nadeem S., Duman H. (2017) Porphyrin-based dye-sensitized solar cells (dsscs): A review. *J. Fluoresc.*, **27**, 1075-1085, <https://doi.org/10.1007/s10895-017-2041-2>
- Semire B., Afolabi S.O., Latona D.F., Oyebamiji A.K., Adeoye M.D., et al (2023) Quantum chemical elucidation on the optoelectronic properties of *n*<sup>2</sup>-(4-aminophenyl)pyridine-2,5-diamine based dyes for solar cells utilization. *Chem. Afr.*, **6**, 2649-2663, <https://doi.org/10.1007/s42250-023-00674-8>
- Thomas S., Deepak T.G., Anjusree G.S., Arun T.A., Nair S.V., et al. (2014) A review: On counter electrode materials in dye-sensitized solar cells. *J. Mater. Chem. A*, **2**, 4474-4490, <https://doi.org/10.1039/C3TA13374E>
- Wu M., Lin X., Wang Y., Wang L., Gu, W., et al. (2012) Economical Pt-free catalysts for counter electrodes of dye-sensitized solar cells. *J. Am. Chem. Soc.*, **134**, 7, 3419-3428, <https://doi.org/10.1021/ja209657v>
- Al-Ezzi A.S., Ansari M.N.M. (2022) Photovoltaic solar cells: A review. *Appl. Syst. Innov.*, **5**, 67. <https://doi.org/10.3390/asi5040067>
- Hara K., Horiguchib T., Kinoshitab T., Sayama K., Sugiharaa H., et al. (2000) Highly efficient photon-to-electron conversion with mercurochrome-sensitized nanoporous oxide semiconductor solar cells. *Solar Energy Materials and Solar Cells*. **64**(2), 115-134. [https://doi.org/10.1016/S0927-0248\(00\)00065-9](https://doi.org/10.1016/S0927-0248(00)00065-9)
- Prihanto T., Sudijito S., Denny W, Lilis Y. (2019) Performance improvement of dye sensitized solar cell (DSSCs) based natural dyes. *Int. J. Photoenergy*, 4384728, <https://doi.org/10.1155/2019/4384728>
- Jamshidvand A., Keshavarzi R., Mirkhani V., et al. (2021) A novel Ru (II) complex with high absorbance coefficient: efficient sensitizer for dye-sensitized solar cells. *J. Mater. Sci: Mater. Electron*, **32**, 9345-9356. <https://doi.org/10.1007/s10854-021-05598-y>
- Ajayi T.J., Ollengo M., le Roux L., Pillay M.N., Staples R.J., et al. (2019). Heterodimetallic ferrocenyl dithiophosphonate complexes of nickel (II), zinc (II) and cadmium (II) as sensitizers for TiO<sub>2</sub>-based dye-sensitized solar cells. *Chemistry*, **25**, 7416-7424, <https://doi.org/10.1002/slct.201900622>
- Cakar S., Özacar M. (2019) The pH dependent tannic acid and Fe-tannic acid complex dye for dye sensitized solar cell applications. *J. Photochem. Photobiol. Chem.*, **371**, 282-291, <https://doi.org/10.1016/j.jphotochem.2018.11.030>
- Anik S., Miftahussurur H.P., Abul Kalam B., Anil K.B., Axel G. (2023) Insight on the choice of sensitizers/dyes for dye sensitized solar cells: A review. *Dyes and Pigments*, **213**, 111087, <https://doi.org/10.1016/j.dyepig.2023.111087>
- Liu Q., Ren P., Wang X., Li Y. (2018) Experimental and theoretical investigation of photoelectrical properties of tetrabromophenol blue and bromoxyleneol blue based solar cell. *J. Nanomater.*, **2018**, 9720595. <https://doi.org/10.1155/2018/9720595>

14. Semire B., Abdulsalami I.O., Latona D.F., Oyebamiji A.K., Owonikoko A.D., et al. (2023) Effect of Seleno-thiophene  $\pi$ -linkers on electronic and photovoltaic properties of boro-phenothiazine donors for DSSCs application: TD-DFT and DFT methods. *Russ. J. Phys. Chem. A*, **98**, 156-168, <https://doi.org/10.1134/S0036024424010217>
15. Mozaffari S., Nateghi M.R., Zarandi M.B. (2017) An overview of the challenges in the commercialization of dye sensitized solar cells. *Renewable and Sustainable Energy Reviews*, **71**, 675-686, <https://doi.org/10.1016/j.rser.2016.12.096>
16. Dindorkar S.S., Yadav A. (2022) Insights from density functional theory on the feasibility of modified reactive dyes as dye sensitizers in dye-sensitized solar cell applications. *Solar*, **2**, 12-31, <https://doi.org/10.3390/solar2010002>
17. Obiyenwa G.K., Semire B., Oyebamiji A.K., Abdulsalami I.O., Latona D.F., et al. (2023) TD-DFT and DFT investigation on electrons transporting efficiency of 2-cyano-2-pyran-4-ylidene-acetic acid and 2-cyanoprop-2-enoic acid as acceptors for thiophene-based  $\pi$ -linkers dye-sensitized solar cells. *Eurasian J. Chem.*, **111**(3), 69-82. <https://doi.org/10.31489/2959-0663/3-23-9>
18. Zdyb A., Krawczyk S. (2014) Adsorption and electronic states of morin on TiO<sub>2</sub> nanoparticles. *Chem. Phys.*, **443**, 61-66. <https://doi.org/10.1016/j.chemphys.2014.08.009>
19. Ibrahim O.A., Bello I.A., Semire B., Bolarinwa H.S., Boyo A. (2016) Purity-performance relationship of anthocyanidins as sensitizer in dye-sensitized solar cells. *Int. J. Phys. Sci.*, **11**(8), 104-111. <https://doi.org/10.5897/IJPS2016.4468>
20. Liu B., Wang R., Mi W., Li X., Yu H. (2012) Novel branched coumarin dyes for dye-sensitized solar cells: significant improvement in photovoltaic performance by simple structure modification. *J. Mater. Chem.*, **22**, 15379-15387, <https://doi.org/10.1039/C2JM32333H>
21. Britel O., Fitri A., Benjelloun A.T. (2023) New carbazole-based dyes for efficient dye-sensitized solar cells: A DFT insight. *Struct. Chem.*, **34**, 1827-1842 <https://doi.org/10.1007/s11224-023-02122-2>
22. William O.A., Obiyenwa K.G., Abubakar M.K., Salawua O.W., Semire B., (2024) Molecular design and optoelectronic investigations of phenothiazine D-A- $\pi$ -A dye sensitizers using DFT/TD-DFT method for potential solar cell application. *Phys. Chem. Res.*, **12**(4), 901-918. <https://doi.org/10.22036/pcr.2024.444731.2482>
23. Semire B., Oyebamiji A.K., Odunola O.A. (2017) Tailoring of energy levels in (2Z)-2-cyano-2-[2-[(E)-2-[2-[(E)-2-(p-tolyl)vinyl]thieno[3,2-b]thiophen-5-yl]vinyl]pyran-4-ylidene]acetic acid derivatives via conjugate bridge and fluorination of acceptor units for effective D- $\pi$ -A dye-sensitized solar cells: DFT-TDDFT approach. *Res. Chem. Intermed.*, **43**, 1863-1879. <https://doi.org/10.1007/s11164-016-2735-0>
24. Hailu Y.M., Pham-Ho M.P., Nguyen M.T., Jiang J.C. (2020) Silole and selenophene-based D- $\pi$ -A dyes in dye-sensitized solar cells: Insights from optoelectronic and regeneration properties. *Dyes Pigm.*, **176**, 108243. <https://doi.org/10.1016/j.dyepig.2020.108243>
25. Akram M., Siddique S.A., Iqbal J., Hussain R., Mehboob M.Y., et al. (2021) End-capped engineering of bipolar diketopyrrolopyrrole based small electron acceptor molecules for high performance organic solar cells. *Comput. Theor. Chem.*, **1201**, 113242
26. Mustafa FM., Abdel-Latif MK., Abdel-Khalek AA., Kühn O. (2023) Efficient D- $\pi$ - $\pi$ -A-type dye sensitizer based on a benzothiadiazole moiety: A computational study. *Molecules*, **28**, 5185. <https://doi.org/10.3390/molecules28135185>
27. Semire B., Obiyenwa K.G., William O.A., Abubakar M.K., Godwin M.A., et al. (2024) Manipulation of 2-[2-(10H-phenothiazin-3-yl)thiophen-3-yl]10H-phenothiazine based D-A- $\pi$ -A dyes for effective tuning of optoelectronic properties and intramolecular charge transfer in dye sensitized solar cells: A DFT/TD-DFT Approach. *Adv. J. Chem. A*, **7**(1), 41-58, <https://doi.org/10.48309/ajca.2024.412442.1400>
28. Afolabi S.O., Semire B., Akiode O.K., Afolabi T.A., Adebayo G.A., et al. (2020) Design and theoretical study of phenothiazinebased low bandgap dye derivatives as sensitizers in molecular photovoltaics. *Opt. Quantum Electron.*, **52**, 476. <https://doi.org/10.1007/s11082-020-02600-5>
29. Salimi Beni A.R., Karami M., Hosseinzadeh B., Ghahary R. (2018) New organic dyes with diphenylamine core for dyesensitized solar cells. *J. Mater. Sci.*, **29**, 6323-6336. <https://doi.org/10.1007/s10854-018-8612-4>
30. Afolabi S.O., Semire B., Idowu M.A. (2021) Electronic and optical properties' tuning of phenoxazine-based D-A2- $\pi$ -A1 organicdyes for dye-sensitized solar cells. DFT/TDDFT investigations. *Heliyon*, **7**(4) e06827. <https://doi.org/10.1016/j.heliyon.2021.e06827>
31. Buene A.F., Boholm N., Hagfeldt A., Hoff B. (2019) Effect of furan  $\pi$ -spacer and triethylene oxide methyl ether substituents on performance of phenothiazine sensitizers in dye-sensitized solar cells. *New J. Chem.*, **43**, 9403-9410. <https://doi.org/10.1039/C9NJ01720H>
32. Ouared I., Rekis M., Trari M. (2021) Phenothiazine based organic dyes for dye sensitized solar cells: A theoretical study on the role of  $\pi$ -spacer. *Dyes Pigm.*, **190**, 109330. <https://doi.org/10.1016/j.dyepig.2021.109330>
33. Consiglio G., Gorczyński A., Petralia S., Forte G. (2023) Predicting the dye-sensitized



- solar cell performance of novel linear carbon chain-based dyes: Insights from DFT simulations. *Dalton Trans.*, **52**, 15995-16004, <https://doi.org/10.1039/D3DT01856C>
34. Casari C.S., Tommasini M., Tykwinski R.R., Milani A. (2016) Carbon-atom wires: 1-D systems with tunable properties. *Nanoscale*, **8**, 4414-4435, <https://doi.org/10.1039/C5NR06175J>
  35. Consiglio G., Gorczyński A., Petralia S. Forte G. (2023b) Computational study of linear carbon chain based organic dyes for dye sensitized solar cells. *RSC Adv.*, **13**, 1019-1030, <https://doi.org/10.1039/D2RA06767F>
  36. Spartan 14 Wavefunction, INC, Irvine, CA. 2015.
  37. Domingo L.R., Ríos-Gutiérrez M., Pérez P. (2016) Applications of the conceptual density functional theory indices to organic chemistry reactivity. *Molecules*, **21**, 748, <https://doi.org/10.3390/molecules21060748>
  38. Liu X., Cole J.M., Low K.S. (2013) Molecular origins of dye aggregation and complex formation effects in coumarin 343. *J. Phys. Chem. C*, **117**, 14723-14730, <https://doi.org/10.1021/jp4024266>
  39. Ren P., Sun C., Shi Y., Song P., Yang Y., Li Y. (2019) Global performance evaluation of solar cells using two models: from charge-transfer and recombination mechanisms to photoelectric properties. *J. Mater. Chem. C*, **7**(7), 1934–1947, <https://doi.org/10.1039/C8TC05660A>
  40. Muhammed K.A., Anthony W.O., Obiyenwa K.G., Salawu O.W., Semire B. (2025) Phenyl-9H-Phenothiazine and phenyl-9H-Phenoxazinebased metal free dye-sensitizers (D-A2- $\pi$ -A1) with thieno[3,4-b]pyrazine auxiliary acceptor for dyesensitized solar cell applications: DFT and TD-DFT computational studies. *J. Sulf. Chem.*, **46**(3), 479-504. <https://doi.org/10.1080/17415993.2025.2463490>
  41. Olatunde A.M., Adedokun N.O., Owonikoko A.D., Obiyenwa G.K., Anthony W.O., et al. (2024) Optoelectronic of properties of  $N^1$ -[4-(diethylamino)phenyl]- $N^4,N^4$ -diethyl- $N^1$ -(thiophen-2-yl)benzene-1,4-diamine-based (D-A2- $\pi$ -A) dyes with enzothiadiazole /dihydrothieno[3,4-b][1,4]dioxine as auxiliary acceptor for DSSCs applications: DFT/TD-DFT approach. *Russ. J. Gen. Chem.*, **94**(10), 2710-2720, <https://doi.org/10.1134/S1070363224100165>
  42. Delgado-Montiel T., Baldenebro-López J., Soto-Rojo R., Glossman-Mitnik D., (2020) Theoretical study of the effect of  $\pi$ -bridge on optical and electronic properties of carbazole-based sensitizers for DSSCs. *Molecules*, **25**, 3670, <https://doi.org/10.3390/molecules25163670>
  43. Abdel Aal S., Awadh D. (2023) The effect of central transition metals and electron-donating substituent on the performances of dye/TiO<sub>2</sub> interface for dye-sensitized solar cells applications. *J. Mol. Graphics Model*, **123**, 108525. <https://doi.org/10.1016/j.jmgm.2023.108525>
  44. Patil D.S., Avhad K.C., Sekar N. (2018) Linear correlation between DSSC efficiency, intramolecular charge transfer characteristics, and NLO properties – DFT approach. *Computational and Theoretical Chem.*, **1138**, 75-83. <https://doi.org/10.1016/j.comptc.2018.06.006>
  45. Kacimi R., Raftani M., Abram T., Azaid A., Ziyat H., et al. (2021) Theoretical design of D- $\pi$ -A system new dyes candidate for DSSC application. *Heliyon*, **7**(6), e07171. <https://doi.org/10.1016/j.heliyon.2021.e07171>
  46. Irfan A. (2013) Quantum chemical investigations of electron injection in triphenylamine-dye sensitized TiO<sub>2</sub> used in dye sensitized solar cells. *Mater. Chem. Phys.*, **142**(1), 238-247. <https://doi.org/10.1016/j.matchemphys.2013.07.011>
  47. Janjua MRSA. (2022) All-small-molecule organic solar cells with high fill factor and enhanced open-circuit voltage with 18.25% PCE: Physical insights from quantum chemical calculations. *Spectrochim. Acta A*, **15**, 279, 121487, <https://doi.org/10.1016/j.saa.2022.121487>
  48. Khan M.U., Abida A.A., Hassan A.U., Alshehri S.M., Sohail A. (2024) DFT simulations of photovoltaic parameters of dye-sensitized solar cells with new efficient sensitizer of indolo[3,2-b]carbazole complexes. *Energy Sci. Eng.*, **12**, 3681-3703. <https://doi.org/10.1002/ese3.1834>